Extendable Hybrid Approach to Detect Conscious States in a CLIS Patient Using Machine Learning

Sophie Adama[1], Shang-Ju Wu[1*], Nicoletta Nicolaou[2,3], Martin Bogdan[1]

[1]Department of Neuromorphe Information Processing, Leipzig University, Augustusplatz 10, 04109 Leipzig, Germany; *adama* | *[*]shanglu* | *bogdan@informatik.uni-leipzig.de*

[2]Medical School, University of Nicosia, Cyprus; *nicolaou.nic@unic.ac.cy*

[3]Centre for Neuroscience and Integrative Brain Research (CENIBRE), University of Nicosia Medical School, Nicosia, Cyprus

SNE 32(1), 2022, 37-45, DOI: 10.11128/sne.32.tn.10596
Received: 2020-11-10 (Selected EUROSIM 2019 Postconference Publication); Revised: 2021-09-08; Accepted: 2021-10-05
SNE - Simulation Notes Europe, ARGESIM Publisher Vienna, ISSN Print 2305-9974, Online 2306-0271, www.sne-journal.org

Abstract. In this study a method for uncovering consciousness in complete locked-in syndrome (CLIS) patients is proposed. The main characteristic of CLIS patients is sufficiently intact cognition, but complete paralysis. It is, thus, vital to develop alternative means of communicating with CLIS patients, and brain-computer interfaces offer a possible platform to do so. A major issue in the study of consciousness in CLIS patients is that there is no certitude regarding their actual state of consciousness. Existing methods provide only a probability of what the states of the patients might be at each moment. This paper proposes a hybrid system based on the combination of complex coherence, sample entropy and Granger causality to uncover the underlying state of consciousness in a CLIS patient from electrocorticography signals. The contribution of each method to the system is determined using machine learning techniques. The aim of the research is to increase the probability of correctly detecting the patients' consciousness states and, ultimately, use that to develop a reliable brain-computer interface-based communication tool.

Introduction

Locked-in syndrome (LIS) is a state where patients are fully conscious but are unable to produce any speech or perform any muscle movements. Although it is not a disorder of consciousness, LIS is frequently misdiagnosed as one. One such a case was a patient who was considered in an unresponsive wakefulness syndrome (UWS) for 20 years [1]. Patients in a LIS state may still be able to move their eye muscles and can, thus, communicate using eye movements. However, even this limited communication becomes impossible when patients enter a complete locked-in state (CLIS) [2], during which it is thought that cognitive function and consciousness are maintained, but all muscle control is lost. Even though no means of communication is available to interact with CLIS patients, some attempts have been made using electroencephalography (EEG) and Near Infrared Spectroscopy (NIRS) [3], but not without controversy [4]. The most important limitation in any such approach is the lack of "ground truth". It is not possible to ascertain the "true" level of consciousness as the patients cannot express their will or answer in any manner.

We present here a general approach that combines different approaches to uncover the state of consciousness in a CLIS patient from continuously recorded electrocorticography (ECoG). The key advantage of this study is that the all-important "ground truth" is accessible and can provide objective means of detecting the presence of consciousness in such patients. We were able to obtain such a "ground truth" from a CLIS patient, who successfully communicated and answered patient-specific questions asked by an investigator using a brain-computer interface system. To the best of our knowledge, there is no other such dataset in existence. Our ultimate goal is to develop a method in order to detect consciousness in CLIS patients to re-establish communication during the time they are conscious.

The paper is organized as follows. The idea behind the general approach is first presented using a modus operandi. The methods that have initially been investigated as part of this approach, namely complex coherence, multiscale entropy and Granger causality, are then described. Preliminary results are presented and discussed, with considerations regarding future development of the proposed approach.

1 Modus Operandi

To uncover the state of consciousness in a CLIS patient from continuously recorded electrocorticography (ECoG) and with a priori knowledge of the "ground truth", we propose the use of a hybrid system incorporating a combination of feature extraction methodologies (in these initial investigations we use complex coherence, multiscale entropy and Granger causality) and machine learning (e.g. reinforcement learning to capture inter-subject variability) to detect the level of consciousness (Figure 1). The proposed system is modular and can, thus, incorporate additional combinations of consciousness detection algorithms to augment detection accuracy.

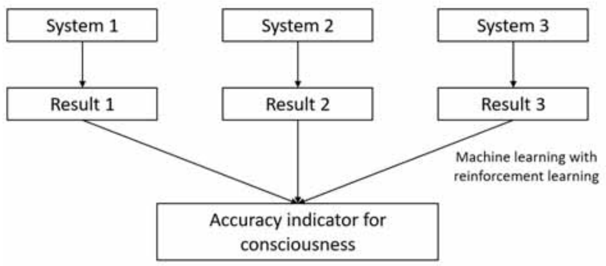

Figure 1: Scheme for the hybrid approach using three different processing systems.

2 Methods

2.1 Dataset

The data was obtained from a 40-year-old male in a complete locked-in state (CLIS). The patient was first diagnosed with amyotrophic lateral sclerosis (ALS) in 1997 and entered CLIS 11 years later [5]. The dataset comprises 24 consecutive one-hour recordings (i.e. 24 hours) of the patient's intracranial brain activity (electrocorticogram - ECoG), acquired with a 64-channel amplifier (BrainAmp from Brainproducts GmbH, Munich, Germany) at a sampling rate of 500 Hz. The ECoG grid electrodes were surgically placed on the patient's left frontal and parietal lobes [1, 6], as shown in Figure 2. The specific channel locations, as well as the locations of the ground and reference electrodes, are also shown in Figure 2.

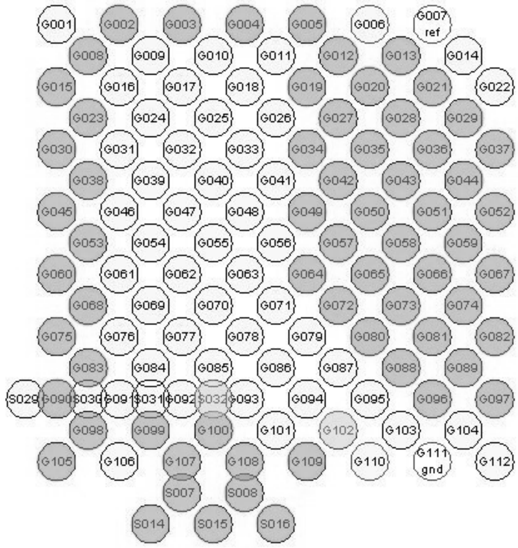

(a)

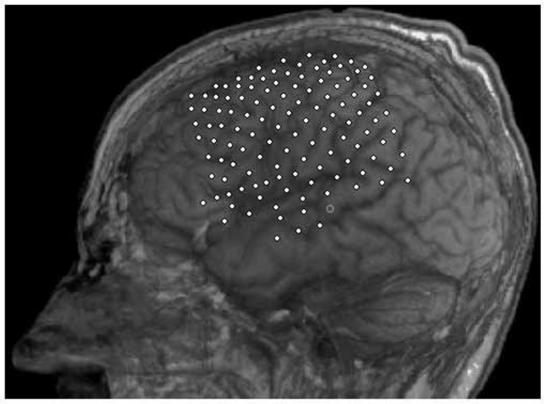

(b)

Figure 2: Channel positions. **(a)** Channel names, with functional recording channels shown in green, and ground and references channels in yellow.
(b) Spatial location of surgically implanted ECoG grid electrodes.

An auditory paradigm similar to [3] was performed from 14:50 to 17:00, in which the patient was asked open questions requiring a "yes" or "no" answer. The questions covered a range of topics such as his mood and feelings and his physiological status, for example: "You feel good today?"/"You feel bad today?" or "Are you German?"/"Are you Dutch?". During the session, a pre-trained classifier was used to give feedback on the predicted answer.

2.2 Feature extraction: Complex coherence

Complex coherence, C_{xy}, at frequency f, of two signals, x and y, is defined as the ratio [7]:

$$C_{xy}(f) = \frac{S_{xy}(f)}{\sqrt{S_{xx}(f) \cdot S_{yy}(f)}} \tag{1}$$

where $S_{xy}(f)$ is the cross power spectral density of the signals, and $S_{xx}(f)$ and $S_{yy}(f)$ is the auto power spectral density of x and y respectively. Coherence is defined as $|C_{xy}(f)|^2$ and is typically used to measure the degree of association between two time series at a specific frequency f. Coherence ranges between 0 and 1.

Coherence has many applications in neuroscience, such as measuring functional relationships between pairs of brain regions. An increased functional interaction between the underlying neuronal networks leads to a higher value of coherence. The complex coherency is to reduce the effects of volume conduction in the brain [8]. Previous researches suggest that the brain waves of locked-in syndrome patients are nearly similar as those of healthy subjects [1]. For that reason, we hypothesize that patients brain rhythms would to some extent behave like the healthy subject's ones.

The data was analysed using MATLAB R2018b (The MathWorks, Natick MA, USA) and custom written codes. Prior to any other processing, the data was re-referenced to the mean and band pass filtered at frequencies 0.5 to 50 Hz using a third order Butterworth filter [9]. The signals were down-sampled to 100 Hz afterwards to reduce the computation time. The signal was subsequently partitioned into segments of 1-second length. Finally, for each frequency band (delta: 0.5-4 Hz, theta: 4-8 Hz, alpha: 8-12 Hz, beta: 12-30 Hz and gamma: 30-50 Hz) and for each time segment, coherency values were computed according to equation (1). A series of coherence matrices were, thus, obtained, each matrix representing the coherence between all pairs of electrodes at each time point. For each of the frequency bands of interest, these sequences were combined to produce a video file, thus facilitating visual inspection of any changes in the coherence over time.

2.3 Feature extraction: Entropy

Entropy is a physical concept, which is related to the total amount of disorder within a system. It can be used for nonlinear dynamic analysis in both the time and frequency domain to quantify the regularity (predictability) of a time series. The family of entropy-based methods is frequently used in neuroscience applications [10, 11, 12].

Sample entropy. Sample Entropy (*SampEn*) is a modification of Approximate Entropy (*ApEn*) proposed by Richman and Moorman [13] to address some of the limitations of *ApEn*. Specifically, the advantages of *SampEn* over *ApEn* are data length independence and non-inclusion of self-matches in the estimation (inclusion of self-matches in *ApEn* result in an interpretation of the signals as more regular than they are). *SampEn* has been used in a number of neuroscience applications, including applications relating to consciousness, such as evaluation of the patient's depth of anaesthesia (DOA) in surgery.

Consider a time series $X = [x(1), x(2), \ldots, x(N)]$, with a total of N samples. To estimate the *SampEn*, the time series is divided into a group of m-dimensional vectors (where m is the embedding dimension), $u_m(1), \ldots, u_m(N-m)$, with $u_m(i) = [x(i), x(i+1), \ldots, x(i+m-1)]$, $i = 1 \ldots N-m+1$. Define the distance, $d[u_m(i), u_m(j)]$, between $u_m(i)$ and $u_m(j)$:

$$d[u_m(i), u_m(j)] = \max|x(i+k) - x(j+k)| : 0 \le k \le m-1 \tag{2}$$

A threshold, $R = r * SD$, where SD is the standard deviation of the time series X and r is the tolerance, is set for the distance. $SampEn(N, m, r)$ is then estimated as

$$SampEn(N, m, r) = -\log \frac{A^m(r)}{B^m(r)} \tag{3}$$

where:

$$B^m(r) = (N-m)^{-1} \sum_{i=1}^{N-m} B_i^m(r) \tag{4}$$

$$A^m(r) = (N-m-1)^{-1} \sum_{i=1}^{N-m} A_i^m(r) \tag{5}$$

B_i^m be the number of vectors for which $d[u_m(i), u_m(j)] < R$, and A_i^m the number of vectors for which $d[u_{m+1}(i), u_{m+1}(j)] < R$. Larger values of *SampEn* indicate reduced self-similarity of the series and increased time series complexity. In contrast, smaller *SampEn* values indicate increased self-similarity and lower complexity. Thus, we are expecting that during periods of increased consciousness the *SampEn* values will be higher. The variables m and r need to be set in advance. Commonly used values for neuroscience applications are $m = 1,...,3$ and $r = 0.1, 0.2$ [13, 14].

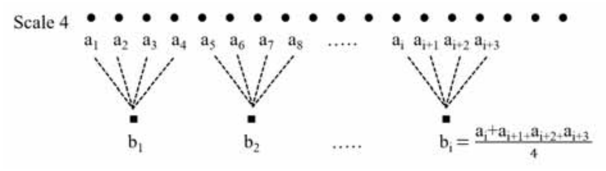

Figure 3: Multiscale Entropy: the coarse-graining procedure for scale 4.

Multiscale entropy. The method of Multiscale Entropy (MSE) analysis is useful for investigating complexity, in contrast to regularity, in signals that have correlations at multiple (time) scales. MSE is an extension of *SampEn* that was proposed by Costa et al. as a way of reducing the effect of white noise that is present in *SampEn* estimations [15, 16]. This is achieved by, first, obtaining a coarse-graining of the data by averaging the data points in non-overlapping windows of increasing length (scale). *SampEn* is then estimated for each coarse-grained series to obtain an index of complexity over multiple time scales. An example of the coarse graining for a scale of 4 is shown in Figure 3.

For the specific dataset, in order to reduce the computation time the original ECoG signals were, first, down-sampled to 125 Hz. Secondly, the down-sampled signals were band pass filtered by a sixth order Butterworth Filter in 1-45 Hz. Finally, the multiscale entropy algorithm is applied to obtain a level of consciousness. For *SampEn* we have set $m = 3$ and $r = 0.2$, and for MSE we have set the scale to 4. Similarly to *SampEn*, higher (lower) values of MSE indicate higher (lower) time series complexity. Thus, we are expecting that periods of consciousness will be characterised by higher MSE values.

We applied sample entropy algorithm and according to the relationship between parameters N and m, the value of N between minimum 10^m and maximum 30^m (when $m = 3$) is chosen [13, 14].

2.4 Granger causality

The concept of causality was first introduced by Wiener [20], as a means of quantifying cause-effect interactions between variables through modelling, prediction and assessment of the goodness-of-fit of models that incorporate the past information from one variable (cause) into the prediction of another variable (effect). Wiener's definition of causality is as follows: *for two simultaneously measured signals, if one can predict the first signal better by incorporating the past information from the second signal than using only information from the first one, then the second signal can be called causal to the first one*. Causality was given a formal mathematical framework by Granger, whereby the goodness-of-fit was assessed through the variance of the residual error of the fitted univariate and bivariate models, i.e. the smaller the residual error variance, the better the fit [21]. The common models of choice for Granger causality are Autoregressive models (AR). For a time series, $X_j = [x_1, x_2, \ldots, x_T]$, a univariate AR model is described by

$$x_j(t) = \sum_{i=1}^{p} a_{ix_j} x_j(t-i) + e_{x_j}(t) \qquad (6)$$

where a_{ix_j} are the estimated univariate AR coefficients for an AR model of order p, and e_{x_j} is the residual (prediction error) of the AR process. Similarly, a bivariate

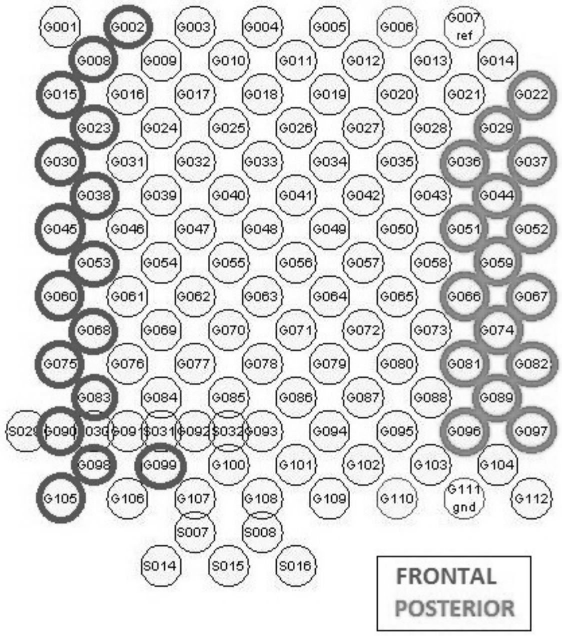

Figure 4: Channels for frontal (blue) and posterior (maroon) aggregate areas.

AR model is given by

$$x_j(t) = \sum_{i=1}^{p} a_{ix_jx_k} x_j(t-i) + \sum_{i=1}^{p} b_{ix_jx_k} x_k(t-i) + e_{x_jx_k}(t) \tag{7}$$

where $a_{ix_jx_k}$, $b_{ix_jx_k}$, and $e_{x_jx_k}$ are the corresponding bivariate AR coefficients and residuals for the bivariate AR model of order p.

By comparing the error variances of the univariate and bivariate AR model residuals, one can then deduce the causality as follows:

$$GC(X_j \rightarrow X_k) = \ln \frac{\sigma^2_{X_j/X_j}}{\sigma_{X_j/(X_j,X_k)}} \tag{8}$$

where $GC(X_j \rightarrow X_k)$ is the Granger causality from X_j to X_k, while $\sigma^2_{X_j/X_j}$ and $\sigma^2_{X_j/(X_j,X_k)}$ are the residual error variances from the univariate and bivariate AR models respectively. By definition, $GC = 0$ when the time series are independent, and $GC > 0$ otherwise. From equation (8) it can be seen that if the univariate AR model is a better fit, then GC will be close to zero. In contrast, if the bivariate model is a better fit, then GC will increase. If GC is high in one direction, this signifies a unidirectional causal relationship; if, however, GC is high in both directions, then a bidirectional causal relationship is inferred.

Causality has been widely applied in the field of neuroscience [22], with a number of applications relating to the study of consciousness. More specifically, it was found that the direction and strength of causal relationships displays distinct changes between wakefulness and lack thereof, induced by either physiological or pharmacological interventions and as captured by EEG activity, with fronto-posterior causal interactions identified as being of paramount importance [22, 23, 24]. The coupling between frontal and posterior areas appears to be an important mechanism for loss of consciousness, as a number of additional functional measures, such as transfer entropy (TE) [25], coherence and cross-dependence also indicate the breakdown of functional connectivity between frontal and posterior structures [26]. Coupling between anterior and posterior brain regions and propagation of EEG activity from fronto-central to posterior regions was also found during deep sleep [27], and breakdown of effective connectivity among specialized thalamocortical modules may underlie the fading of consciousness in deep sleep [28].

Even though GC is traditionally defined for pairwise relationships, there are some limitations that must be considered (see Bressler and Seth for a detailed review [29]). For example, it is not possible to distinguish between direct and indirect causal relationships when performing pairwise GC analysis. This is related to the issue of spurious causality that can appear between two processes when both are influenced by external sources that are not taken into account [30]. In order to infer a more precise structural causality, in theory one must include all sources of influence into the estimation. However, in practice this is unfeasible and even though multivariate versions of causality exist, these minimise the effects rather than eliminate them completely. Wang and colleagues have shown that both pairwise and blockwise approaches to GC estimation give consistent results [23]. As such, pairwise time-domain GC analysis still remains a valid methodology, particularly when a blockwise approach is taken (i.e. the two time series are aggregate activity from a number of individual time series or the GC is itself an aggregate of a number of pairwise GC estimates). An additional consideration relating to AR modelling is the issue of stationarity. Given that AR models assume a stationary process, nonstationary EEG signals must be analyzed in windows of short duration. It is widely accepted that EEG exhibits stationary properties for segments less than 20 seconds [31]. Therefore, common practice involves EEG analysis in short segments.

Taking into account the above considerations and related studies, the EEG was analysed in 4-s windows, overlapping by 2-s. For each 4-s segment, GC was estimated for aggregate activity from “frontal” and “posterior” areas, consisting of the channels indicated in Figure 4.

3 Results

The main purpose of the investigations was to compare and contrast the ability of different methods, which have commonly been applied in neuroscience applications, to correctly indicate periods of consciousness in a CLIS patient corresponding to the "ground truth" known *a priori*.

3.1 Imaginary coherence

Figure 5 shows an example coherence matrix obtained for all combinations of the 64 ECoG channels. A visual inspection of the resulting coherence matrices videos

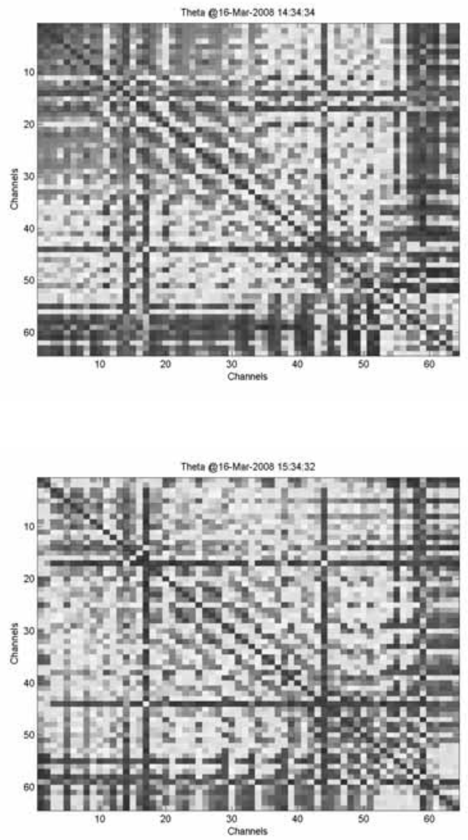

(a)

(b)

Figure 5: Coherence matrices of theta rhythms **(a)** during unconsciousness; **(b)** during consciousness.

indicates changes in coherence in distinct directions. To assess these direction changes further analysis was performed using artificial neural networks [32]. These changes across time are shown in Figure 6. On the other hand, analysis on the coherence value between each pair of channels across time revealed interesting variations in the higher frequencies in some channels (cf. Figure 6). The combination of the obtained results suggests an interesting change of state around 15:15-15:30 to 16:00-16:10. This corresponds to the time window during which the CLIS patient was consciously responding to the investigator's questions, as reported by the investigator.

3.2 Sample entropy

Multiscale sample entropy applied to analyze the cognition state in time domain. The higher multiscale sample

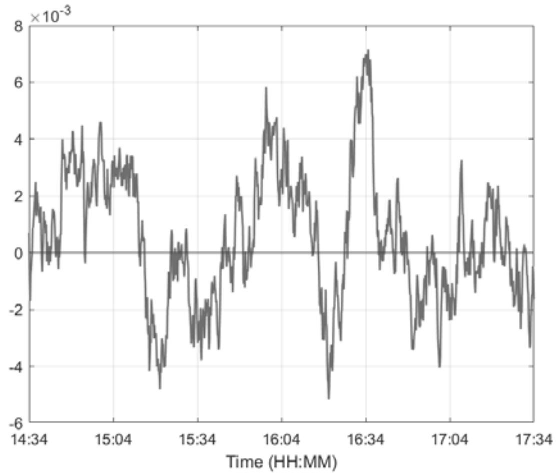

Figure 6: Motion direction changes in the theta bands.The x-axis represents the time and the y-axis represent the direction changes.

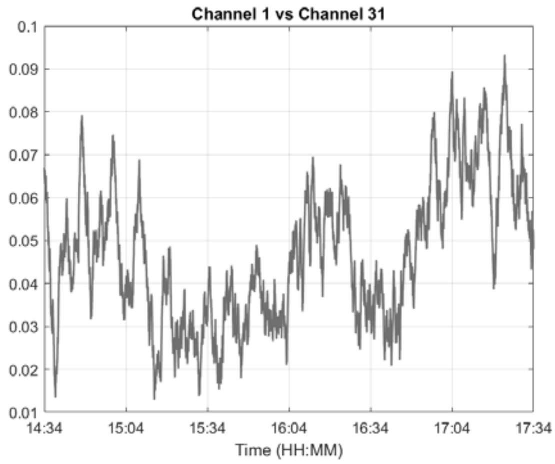

Figure 7: Coherence between one frontal and one parietal channel. There is a distinguished decrease of value between 15:10 and 16:10, and from 16:30 to around 16:45.

entropy means more indicated for consciousness. Figure 8 shows the result is the average from all usable channels, shows that the value of multiscale sample entropy relative high in the period between 15:24-16:14. This period coincides with the time window during the experiment in which the investigators receive feedback from CLIS patients.

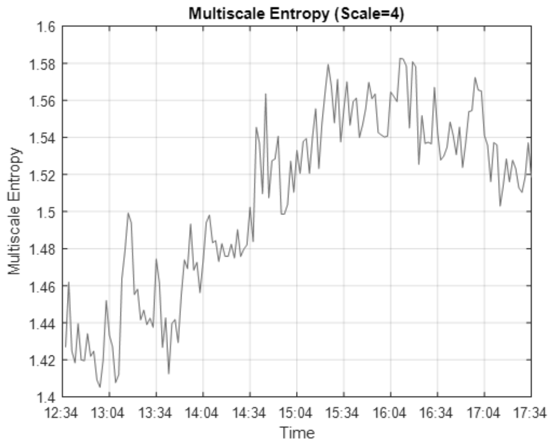

Figure 8: The result of Multiscale Entropy.

3.3 Granger causality

Figure 9 shows the estimated fronto-posterior GC in the evaluation of the state of the locked-in patient based on the recorded brain activity. Findings reported in the literature regarding the patterns of GC during wakefulness and unconsciousness suggest that a unidirectional increase in fronto-posterior GC is indicative of loss of consciousness. Based on these findings, the GC pattern observed during the period of 15:34 – 16:14 pm suggests that the patient is awake during this period. This period matches the period during which the CLIS patient was reported to have been communicating with the investigator. Similar patterns of reduced fronto-posterior GC can also be seen at various time points in Figure 9, which seems suggestive of additional transient periods of awareness.

4 Discussion

The methods presented here suggest a measurable change of the consciousness level occurring approximately between 15:15-16:45. This coincides with the period during which the CLIS patient was reported to have been communicating with the investigator via a brain-computer interface [5]. The probability of detecting changes in the consciousness level of the CLIS patient can, thus, be increased by combining the results of these methods. Such combination will reduce the uncertainty that is inherent to characterisation of the level of consciousness of CLIS patients, for which the "ground truth" is rarely available.

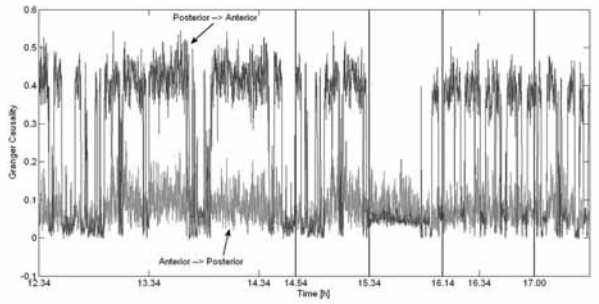

Figure 9: Fronto-posterior GC. A pattern of increased unidirectional fronto-posterior GC suggests unconsciousness, while a reduced bidirectional fronto-posterior GC suggests wakefulness. A long period of wakefulness, as well as several periods of transient wakefulness, can be identified.

5 Conclusion

In this paper, three approaches to detect conscious state in a complete locked-in patient were presented. These approaches will be combined in a hybrid approach with machine learning in a brain-computer interface system to ultimate establish a means of communication with CLIS patients. The combination of the different approaches should increase the probability of correctly detecting the patient's state. Based on the data set used in this paper, it has not only been shown even though different methods reporting different time slice each, but all around the same time slice the experimenter confirmed consciousness of the patient, the certainty of correctness of consciousness can be augmented by combing these three systems into one answer leading to the whole time slice reported by the experimenter judging the CLIS patient conscious.

Acknowledgement

Data was kindly provided by Prof. Dr. Dr. hc. mult. Niels Bierbaumer from the Institute for Medical Psychology and Behavioural Neurobiology, University of Tübingen.

References

[1] Vanhaudenhuyse A, Charland-Verville V, Thibaut A, Chatelle C, Tshibanda JFL, Maudoux A. Conscious While Being Considered in an Unresponsive Wakefulness Syndrome for 20 Years. *Front. Neurol.*. 2018; 9: 671. doi: 10.3389/fneur.2018.00671.

[2] Laureys S, Tononi G. *The neurology of consciousness. Cognitive neuroscience and neuropathology*. 2nd edn. Amsterdam, London: Academic; 2009. 440 p.

[3] Chaudhary U, Xia B, Silvoni S, Cohen LG, Birbaumer N. Brain–Computer Interface–Based Communication in the Completely Locked-In State. *PLoS Biol*. 2017; 15(1): page–page. doi: 10.1371/journal.pbio.1002593.

[4] Spueler M. Questioning the evidence for BCI-based communication in the complete locked-in state. *PLOS Biol*. 2019; doi: 10.1371/journal.pbio.2004750.

[5] Murguialday AR, Hill J, Bensch M, Martens S, Halder S, Nijboer F. Transition from the locked in to the completely locked-in state: A physiological analysis. *Clinical Neurophysiology*. 2011; 122(5): 925–933. doi: 10.1016/j.clinph.2010.08.019.

[6] Soekadar SR, Born J, Birbaumer N, Bensch M, Halder S, Murguialday AR. Fragmentation of slow wave sleep after onset of complete locked-in state. *Journal of clinical sleep medicine (JCSM)*. 2013; 9(9): 951–953. doi: 10.5664/jcsm.3002.

[7] Priestley, MB. *Spectral analysis and time series*. Probability and mathematical statistics. Academic Press; 1989. 890 p.

[8] Nolte G, Bai O, Wheaton L, Mari Z, Vorbach S, Hallett M. Identifying true brain interaction from EEG data using the imaginary part of coherency. *Clinical Neurophysiology*. 2004; 115(10): 2292–2307. doi: 10.1016/j.clinph.2004.04.029.

[9] Cohen, MX. *Analyzing neural time series data. Theory and practice*. Issues in clinical and cognitive neuropsychology. Cambridge, Massachusetts: The MIT Press; 2014. 600 p.

[10] Yeragani V. K., Pohi R., Mallavarapu M., Balon R. Approximate entropy of symptoms of mood: an effective technique to quantify regularity of mood. *Bipolar Disord*. 2003; 5: 279–286. doi: 10.1034/j.1399-5618.2003.00012.x .

[11] Diambra L, de Figueiredo JC, Malta CP. Epileptic activity recognition in EEG recording. *Phys A*. 1999; 273: 495–505. doi: 10.1016/S0378-4371(99)00368-4.

[12] Courtiol J, Perdikis D, Petkoski S, Muller V, Huys R, Sleimen-Malkoun R, Jirsa VK. The multiscale entropy: Guidelines for use and interpretation in brain signal analysis. *Journal of Neuroscience Methods*. 2016; 273: 175–190. doi: 10.1016/j.jneumeth.2016.09.004.

[13] Richman JS, Moorman JR. Physiological time-series analysis using approximate entropy and sample entropy. *Am J Physiol Heart Circ Physiol*. 2000; 278: H2039–H2049. doi: 10.1152/ajpheart.2000.278.6.H2039.

[14] Pincus SM, Goldberger AL. Physiological time-series analysis: what does regularity quantify?. *Am J Physiol Heart Circ Physiol*. 1994; 266: H1643–H1656. doi: 10.1152/ajpheart.1994.266.4.H1643.

[15] Costa M, Goldberger AL, Peng CK. Multiscale entropy analysis of biological signals. *Phys Rev E*. 2005; 71.

[16] Costa M, Goldberger AL, Peng CK. Multiscale entropy analysis of physiologic time series. *Phys Rev Lett*. 2002; 89.

[17] Wu SJ, Chen NT, Jen KK, Fan SZ. Analysis of the Level of Consciousness with Sample Entropy a comparative study with Bispectral Index. *European Journal of Anaesthesiology*. 2015; 32: 11.

[18] Wu SJ, Chen NT, Jen KK. Application of Improving Sample Entropy to Measure the Depth of Anesthesia. In *2014 International Conference on Advanced Manufacturing (ICAM)*; 2014; Chiayi, Taiwan.

[19] Wu SJ, Chen NT, Jen KK, Shieh JS, Fan SZ. The Physiological Signals EEG, ECG, and SpO2 are Applied to Analyze the Consciousness and Anesthesia Depth. *AMPT*. 2013; Taipei.

[20] Wiener, N. The theory of prediction. In: E. Beckenbach (eds). *Modern Mathematics for the Engineer*. New York, NY: McGraw-Hill; 1956. p 165–190.

[21] Granger CWJ. Investigating causal relations by econometric models and cross-spectral methods. *Econometrica*. 1969; 37: 424–438. doi: 10.1017/CBO9780511753978.002.

[22] Nicolaou N, Georgiou J. Spatial analytic phase difference of EEG activity during anesthetic-induced unconsciousness. *Clin Neurophysiol*. 2014; 125: 2122–2131. doi: 10.1016/j.clinph.2014.02.011.

[23] Nicolaou N, Georgiou J. Neural Network based classification of anesthesia / awareness using Granger Causality features. *Clinical EEG and Neuroscience*. 2014; 45(2): 77–88. doi: 10.1177/1550059413486271.

[24] Ku SW, Lee U, Noh GJ, Jun IG, Mashour GA. Preferential Inhibition of Frontal-to-Parietal Feedback Connectivity Is a Neurophysiologic Correlate of General Anesthesia in Surgical Patients. *PLOS ONE*. 2011; 6(10): e25155. doi: 10.1371/journal.pone.0025155.

[25] Imas OA, Ropella KM, Douglas Ward B, Wood JD, Hudetz AG. Volatile anesthetics disrupt frontal-posterior recurrent information transfer at gamma frequencies in rat. *Neuroscience Letters*. 2005; 387: 145–150. doi: 10.1016/j.neulet.2005.06.018.

[26] Lee U, Kim S, Noh GJ, Choi BM, Hwang E, Mashour GA. The directionality and functional organization of frontoparietal connectivity during consciousness and anesthesia in humans. *Conscious Cogn*. 2009; 18: 1069–1078. doi: 10.1016/j.concog.2009.04.004.

[27] Kamiński M, Blinowska K, Szelenberger W. Topographic analysis of coherence and propagation of EEG activity during sleep and wakefulness. *Electroen Clin Neuro*. 1997; 102: 216–227. doi: 10.1016/S0013-4694(96)95721-5.

[28] Massimini M, Ferrarelli F, Huber R, Esser SK, Singh H, Tononi G. Breakdown of Cortical Effective Connectivity During Sleep. *Science*. 2005; 309: 2228–2232. doi: 10.1126/science.1117256.

[29] Bressler SL, Seth AK. Wiener-Granger causality: a well established methodology. *Neuroimage*. 2011; 58: 323–329. doi: 10.1016/j.neuroimage.2010.02.059.

[30] Granger CWJ. Testing for causality: a personal viewpoint. *J Econ Dyn Control*. 1980; 2: 329–352. doi: 10.1016/0165-1889(80)90069-X.

[31] da Silva FL. EEG analysis: theory and practice. In: Niedermeyer E, da Silva FL, editors. *Electroencephalography: Basic Principles, Clinical Applications, and Related Fields*. Philadelphia, PA: LWW; 2005. p 1199–1232.

[32] Adama VS, , Blankenburg A., Ernst C., Kummer R., Murugaboopathy S., Bogdan M. Motion Detection in Videos of Coherence Matrices in order to detect Consciousness States in CLIS-patients – an Approach. In *10th EUROSIM Congress on Modelling and Simulation*; 2019 July; Logrono, Spain.